ELSEVIER

Biochemical Pharmacology 64 (2002) 67–77

Biochemical Pharmacology

NMR and pattern recognition studies on liver extracts and intact livers from rats treated with α-naphthylisothiocyanate

Nigel J. Waters[a], Elaine Holmes[a], Catherine J. Waterfield[b], R. Duncan Farrant[c], Jeremy K. Nicholson[a,*]

[a]*Division of Biomedical Sciences, Biological Chemistry, Sir Alexander Fleming Building, Imperial College, London SW7 2AZ, UK*
[b]*Preclinical Safety Sciences, GlaxoSmithKline Research & Development, Ware, Hertfordshire, SG12 ODP, UK*
[c]*Analytical Technologies, GlaxoSmithKline R&D, Stevenage, Hertfordshire, SG1 2NY, UK*

Received 25 September 2001; accepted 5 April 2002

Abstract

The metabolite profiles from livers of toxin-treated rats were investigated using high resolution ^{1}H NMR spectroscopy of aqueous (acetonitrile/water), lipidic (chloroform/methanol) extracts and magic angle spinning (MAS)-NMR spectroscopy of intact tissue. Rats were treated with the model cholestatic hepatotoxin, α-naphthylisothiocyanate (ANIT, 150 mg/kg) and NMR spectra of liver were analysed using principal components analysis (PCA) to extract novel toxicity biomarker information. ^{1}H NMR spectra of control aqueous extracts showed signals from a range of organic acids and bases, amino acids, sugars, and glycogen. Chloroform/methanol extracts showed signals from a range of saturated and unsaturated triglycerides, phospholipids and cholesterol. The MAS ^{1}H NMR spectra of livers showed a composite of signals found in both aqueous and lipophilic extracts. Following ANIT treatment, ^{1}H NMR-PCA of aqueous extracts indicated a progressive reduction in glucose and glycogen, together with increases in bile acid, choline, and phosphocholine signals. ^{1}H NMR-PCA of chloroform/methanol extracts showed elevated triglyceride levels. The ^{1}H MAS-NMR-PCA analysis allowed direct detection of all of the ANIT-induced tissue perturbations revealed by ^{1}H NMR of extracts, enabling metabolic characterisation of the lesion, which included steatosis, bile duct obstruction and altered glucose/glycogen metabolism. MAS-NMR spectroscopy requires minimal sample preparation and, unlike ^{1}H NMR spectroscopy of tissue extracts, does not discriminate metabolites based on their solubility in a particular solvent and so this is a particularly useful exploratory tool in biochemical toxicology.

Keywords: α-Naphthylisothiocyanate; Magic angle spinning; MAS ^{1}H NMR spectroscopy; Liver; Han–Wistar rat; Metabonomics; Aqueous extract; Chloroform/methanol extract

1. Introduction

High resolution ^{1}H magic angle spinning (MAS)-NMR spectroscopy promises to be a powerful technique for investigating the metabolic state of various intact tissues in the areas of drug toxicology [1–3] and disease diagnosis [4,5]. For nonrigid solid materials or highly viscous liquids, high resolution ^{1}H MAS-NMR spectroscopy offers an approach whereby some of the major line broadening contributions attributable to restricted molecular motion and field inhomogeneity in biological tissues are reduced considerably [6]. High resolution ^{1}H NMR spectroscopic studies on extracts of excised tissues, normally requiring relatively large amounts of tissue (>0.25 g), are usually extracted *via* protein precipitation methods to enable the collection of high resolution spectra without interference from cellular proteins. MAS-NMR spectroscopy of tissues is nondestructive, requires no sample preparation and additionally allows molecular compartmentation and dynamic interactions to be investigated [3,7–12].

The ^{1}H MAS-NMR spectroscopy has recently been applied to the study of whole tissues such as renal cortex and liver [7–9], adipose tissue [11], intact red blood cells [10], prostate [5], and brain [4]. Procedures involved in this technique have been optimised for many of these tissues to validate the information gained from such MAS-NMR

* Corresponding author. Tel.: +44-207-594-3195; fax: +44-207-594-3226.
E-mail address: j.nicholson@ic.ac.uk (J.K. Nicholson).

Abbreviations: ANIT, α-naphthylisothiocyanate; CPMG, Carr–Purcell–Meiboom–Gill; D_2O, ^2H_2O; FID, free induction decay; GSH, glutathione; MAS, magic angle spinning; NMR, nuclear magnetic resonance; PCA, principal components analysis; TMAO, trimethylamine-*N*-oxide; TSP, 3-(trimethylsilyl)[2,2,3,3-$^2H_4$] propionate.

0006-2952/02/$ – see front matter
PII: S0006-2952(02)01016-X

studies of toxicological episodes and disease processes [7]. We have recently reported the capabilities of an ''integrated metabonomic approach'' to studies of drug toxicology, combining NMR-pattern recognition (PR) studies on urine, plasma and MAS-NMR of liver, using the model cholestatic hepatotoxin α-naphthylisothiocyanate (ANIT) as an example [1]. Prominent features of acute ANIT hepatotoxicity include bile duct epithelial cell necrosis, cessation of bile flow, hepatic parenchymal cell injury and hyperbilirubinaemia [13–15]. Periportal injury is characterised by cholangiolitic hepatitis; inflammation of the liver and biliary capillaries, mediated by portal oedema and neutrophil infiltration. As an extension of this work, we present here a direct comparison of ^{1}H MAS-NMR spectroscopic analyses of control and toxin-treated intact liver tissue with ^{1}H NMR spectroscopic analyses of aqueous and chloroform/methanol liver extracts using PR methods. In particular we aimed to evaluate the differential contributions of a range of chemical classes to the different types of NMR spectra and their associated sample processing procedures to determine which approach is optimal for recovery of pathological information.

2. Materials and methods

2.1. Animal handling and tissue preparation

Thirty-five male Han–Wistar rats were acclimatised for 13 days in plastic cages prior to group allocation and treatment. Animals were transferred to individual metabolism cages in a well-ventilated room at a temperature of 21 ± 2° and a relative humidity of 50 ± 10%, with a 12/12 light/dark cycle. Food (Rat & Mouse No. 1 Diet, Special Diet Services Ltd., Cambridge, UK) and tap water were provided *ad lib.* throughout the study. Body weights were measured daily. Each rat received either a single dose of ANIT in corn oil (p.o. 150 mg/kg, N = 25) or corn oil only (p.o. 10 mL/kg, N = 10). Animals were sacrificed (N = 5) by exsanguination from the abdominal aorta under isoflurane anaesthesia at 3, 7, 24, 31, and 168 hr after dosing with ANIT, and vehicle-dosed control animals at 24 and 31 hr p.d. Triplicate samples of the left lateral lobe of the liver, weighing between 15 and 23 mg, were excised and immediately snap-frozen in liquid nitrogen. Another larger section of the left lateral lobe was snap-frozen for tissue extraction. These samples were stored at −70° until NMR spectroscopic analysis.

2.2. ^{1}H MAS-NMR spectroscopic analysis of intact liver tissue

Samples were rinsed in 0.9% saline D_2O, placed in zirconia 4 mm diameter rotors (Bruker Analytische GmbH, Rheinstetten, Germany) and analysed by ^{1}H MAS-NMR spectroscopy at 600.13 MHz using a Bruker Avance 600 spectrometer operating at 600.13 MHz at an MAS rotor spin rate of 6000 Hz [7]. The MAS-NMR spectra were acquired at 283 K, as measured using a thermocouple system and maintained at this temperature *via* the cooling of the inlet gas pressures responsible for sample spinning. The exact *in situ* temperature was calculated using an internal glucose thermometer; the chemical shifts of the water resonance (temperature sensitive) and the α-anomeric proton of glucose (temperature insensitive) averaged 288 K [16]. For each sample, 128 transients were collected into 32 K data points using a water presaturation pulse sequence (D–90°–t_1–90°–t_m–90°–acquire FID). A secondary irradiation field was applied at the water frequency during the relaxation delay of 3 s and during the mixing period t_m (100 ms), with t_1 fixed at 3 μs. A spectral width of 12,000 Hz and an acquisition time per scan of 1.36 s were used. The 1D Carr–Purcell–Meiboom–Gill (CPMG) spin echo pulse sequence [90°–(τ–180°–τ)$_N$ acquisition] (r = 200 μs, N = 200) with standard presaturation of the water resonance, using a fixed total spin–spin relaxation delay (2Nτ) of 80 ms was applied to measure spin-echo ^{1}H MAS-NMR spectra on all samples. The standard CPMG spin-echo pulse sequence allows a certain degree of spectral editing by the attenuation of signals arising from components with short ^{1}H T_2 relaxation times.

2.3. ^{1}H NMR spectroscopy of extracted liver tissue

Samples of liver tissue (~250 mg) taken from the left lateral lobe were homogenised in 2 mL of 50% acetonitrile in an ice/water bath. The homogenates were centrifuged at 5070 *g* for 5 min at 4°. The supernatants were removed and lyophilised before being reconstituted in 1 mL D_2O. 2 mL of 75% chloroform/25% methanol was added to the pellets and extraction was followed by a further centrifugation (5070 *g* for 15 min at 4°). The lipophilic supernatants were removed, dried under a stream of nitrogen and reconstituted in 500 μL of 75% $CDCl_3$/25% CD_3OD. The reconstituted solutions were transferred to 5 mm (o.d.) NMR tubes together with 0.1% 3-(trimethylsilyl)[2,2,3,3-$^2H_4$] propionate (TSP, an internal standard, chemical shift δ 0.0) and 1% sodium azide (bacteriostatic agent) in D_2O. ^{1}H NMR spectra were acquired on each sample at 600.13 MHz on a Bruker Avance spectrometer at ambient probe temperature (298 K). 1D single pulse experiments were carried out using the standard pulse sequence to achieve satisfactory water suppression in the aqueous extracts (as described previously). For each sample, 128 transients were collected into 64 K data points with a relaxation delay of 2 s and a mixing period of 100 ms. A spectral width of 9600 Hz and an acquisition time per scan of 3.41 s were used.

2.4. Automatic data reduction of NMR spectra and principal components analysis (PCA)

Single pulse and CPMG (MAS-) NMR spectra were data reduced using the program AMIX (Bruker Analytische GmbH, Rheinstetten, Germany). The spectral region

δ 0.2–10.0 was segmented into regions of 0.04 ppm width giving a total of 245 integrated regions per NMR spectrum. The area for each segmented region was expressed as an integral value resulting in an intensity distribution description of the whole spectrum with 245 variables prior to PCA analysis. The region of the spectrum, which included water (δ 4.8–5.4), was removed from the analysis for all intact liver and aqueous extract NMR spectra to eliminate residual spectral artefacts from the incompletely suppressed solvent. For the aqueous liver extracts, the region of the spectrum containing a residual acetonitrile signal (δ 2.08) was also removed from all spectra and for the chloroform/

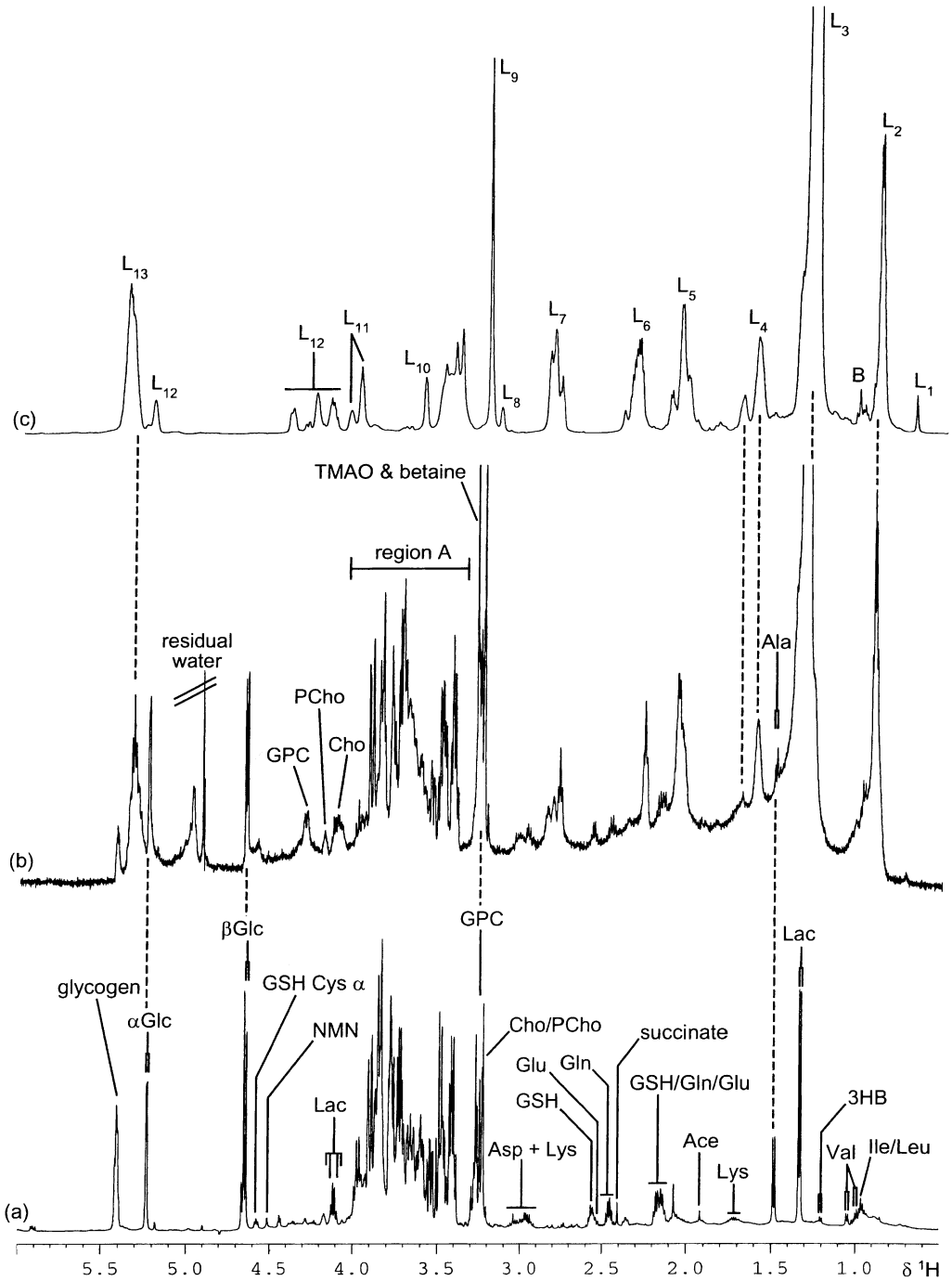

Fig. 1. Series of 600 MHz single pulse ^{1}H NMR spectra (δ 0.5–6.0) of control liver taken from one individual: (a) liver tissue aqueous extract, (b) single pulse ^{1}H MAS-NMR spectrum of intact control liver after Lorentzian–Gaussian function, and (c) liver tissue chloroform/methanol extract. Key: 3HB, 3-D-hydroxybutyrate; Ace, acetate; Ala, alanine; Asp, aspartate; B, C21 bile acid methyl; Cho, choline; Glc, glucose; Gln, glutamine; Glu, glutamate; GPC, glycerophosphorylcholine; GSH, glutathione; Ile, isoleucine; L_1, C18/C19 cholesteryl methyls; L_2, triglyceride terminal methyls; L_3, lipid $(CH_2)_n$; L_4, lipid $CH_2{}^*CH_2CO$, L_5, lipid $CH_2C{=}C$; L_6, lipid CH_2CO; L_7, lipid $C{=}CCH_2C{=}C$; L_8, lipid $CH_2NH_3{}^+$; L_9, lipid $N^+(CH_3)_3$; L_{10}, lipid $(CH_3)_3{}^{N+}CH_2{}^*$; L_{11}, lipid $CH_2OPO_2{}^-$; L_{12}, lipid CH_2OCOR; L_{13}, lipid CH=CH; Lac, lactate; Leu, leucine; Lys, lysine; NMN, *N*-methyl nicotinamide; PCho, phosphocholine; glycogen; TMAO, trimethylamine-*N*-oxide; Val, valine. $^*\alpha$CH resonances of amino acids.

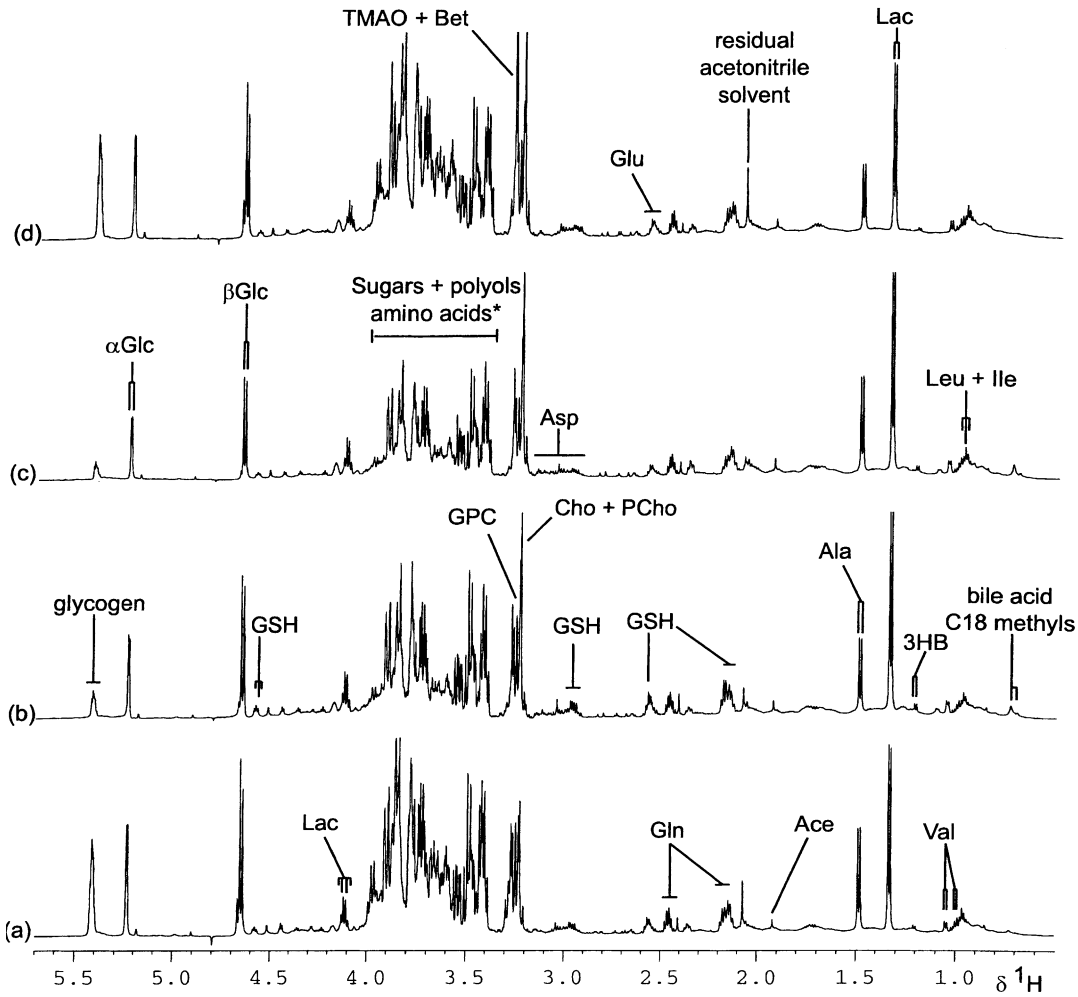

Fig. 2. Series of 600 MHz single pulse ^{1}H NMR spectra (δ 0.5–5.7) of liver tissue aqueous extracts (left lateral lobe) at various time-points following the administration of ANIT (150 mg/kg): (a) control, (b) 24 hr, (c) 31 hr, and (d) 168 hr postdose. Key: As for Fig. 1 with the following additions Bet, betaine.

methanol liver extracts, the regions δ 3.3–3.9 (residual water and methanol) and δ 7.3 (chloroform) were removed from all spectra. Prior to PCA, all remaining spectral segments were scaled to the total integrated area of each spectrum [17]. In addition, the aromatic region (δ 6.0–10.0) of the aqueous liver extract spectra were segmented, integrated and normalised for separate PCA analysis. In order to directly compare the metabolite information obtained by MAS-NMR vs. conventional NMR of extracts, both the aqueous and chloroform/methanol liver extract

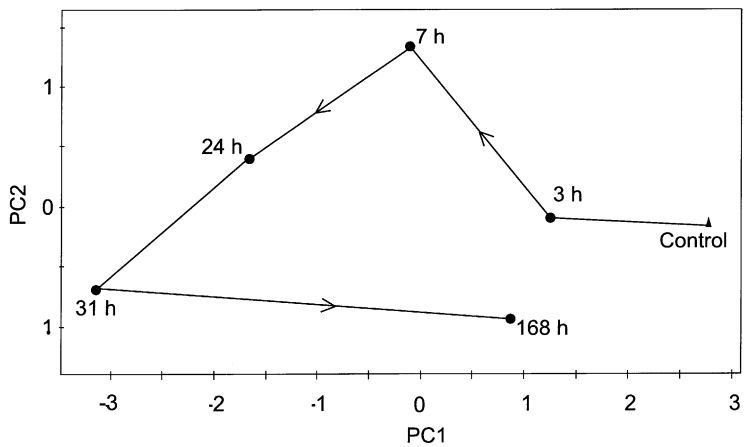

Fig. 3. PC mean trajectory plot showing the average mapping position of aqueous liver tissue extract ^{1}H NMR spectra obtained from individuals following treatment with corn oil (control) or ANIT at various time-points postdose.

normalised spectral datasets (δ 0.5–5.5) were combined as one data matrix prior to PCA analysis.

The single pulse and CPMG ^{1}H NMR spectral data sets were imported into the SIMCA-P8.0 software package (Umetrics AB, Umea, Sweden) separately. These data were then mean centred to zero prior to PCA. With mean-centring, the average value of each variable is calculated and then subtracted from the data. PCA methods involve the calculation of linear combinations of the original descriptors, the PC's, such that each PC is orthogonal to all others, with the first PC (PC1) containing the largest amount of variance with subsequent PC's containing progressively less variance [18,19]. Thus, a scores plot of PC1 vs. PC2 provides the most efficient 2D representation of the information contained in the data set. PCA data were also presented as mean trajectory plots, where each point represents the average position of all animals in a particular group for a given sampling point. Further information can be extracted

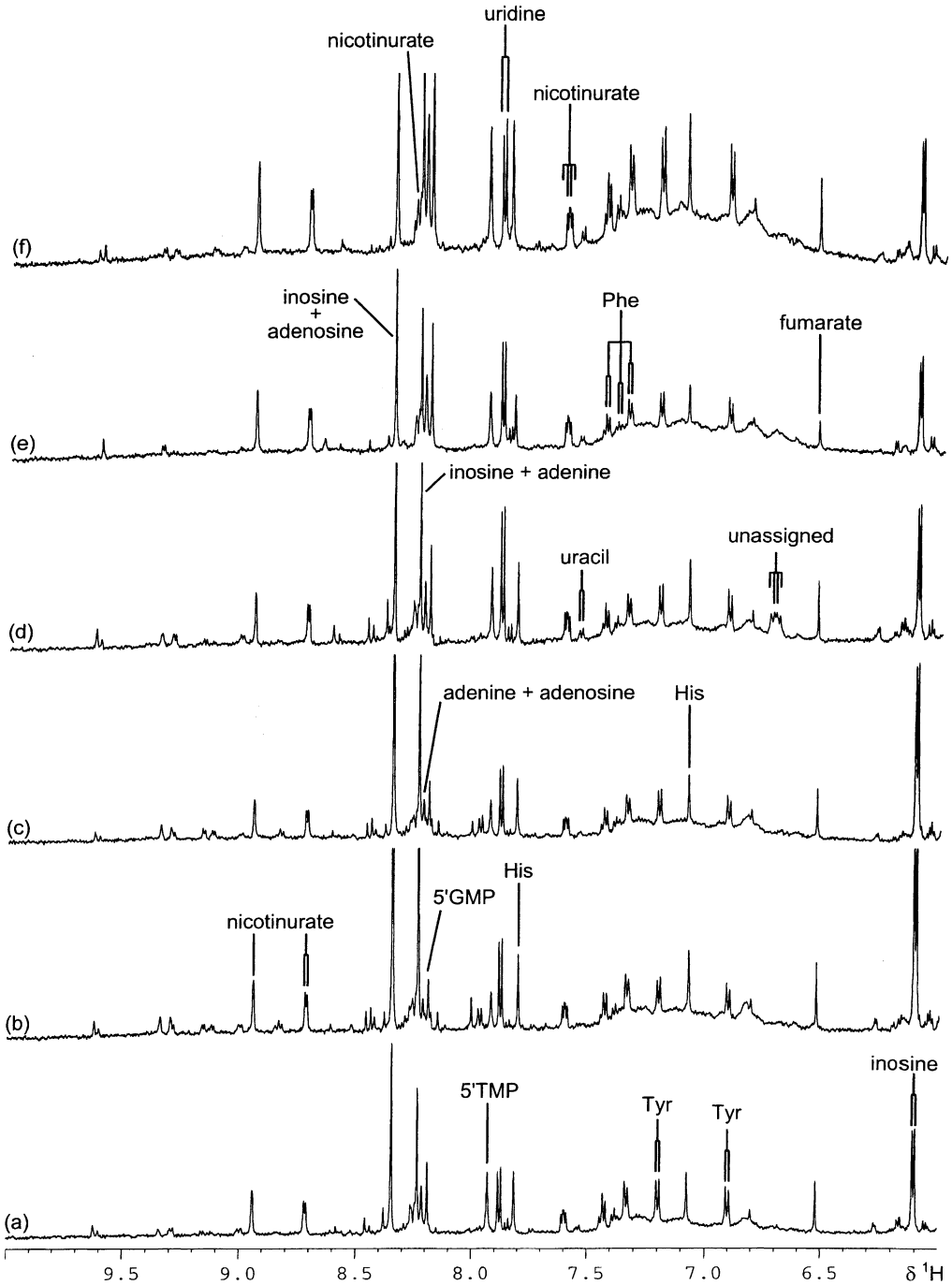

Fig. 4. Series of 600 MHz single pulse ^{1}H NMR spectra (δ 6.0–10.0) of liver tissue aqueous extracts (left lateral lobe) at various time-points following the administration of ANIT (150 mg/kg): (a) control, (b) 3 hr, (c) 7 hr, (d) 24 hr, (e) 31 hr, and (f) 168 hr postdose. Key: As for Fig. 1 with the following additions His, histidine; Phe, phenylalanine; Tyr, tyrosine.

from the dataset by connecting the average coordinates in a time sequence to form a trajectory where the direction of deviation from the control position is indicative of the nature of the lesion, and the magnitude of change from the control position is related to the severity of the lesion [20].

3. Results and discussion

3.1. Biochemical comparison of control intact and extracted liver by ^{1}H NMR spectroscopic techniques

High resolution solution-state ^{1}H NMR spectroscopy of liver extracts, both aqueous and lipophilic, produced characteristic metabolite profiles distinct from high resolution ^{1}H MAS-NMR spectra of intact liver. Extraction of liver tissue using acetonitrile and water led to spectra containing signals from various organic acids and bases, amino acids, sugars and the complex polysaccharide, glycogen (Fig. 1a). On the other hand, extraction of liver tissue with chloroform and methanol gave spectra that were dominated by signals from a variety of lipid moieties including saturated and unsaturated triglycerides, phospholipids and cholesterol (Fig. 1c). The representative ^{1}H MAS-NMR spectrum of intact liver (Fig. 1b) contains a combination of the signals found in both the aqueous and lipophilic extracts. The majority of metabolites observed by ^{1}H NMR spectroscopic analysis of extracts are visible in the 1D ^{1}H MAS-IMR spectra of intact tissue.

High resolution ^{1}H MAS-NMR spectroscopy of intact tissue allows the measurement of cellular metabolites whilst maintaining a significant degree of structural integrity of the tissue and thus potentially allows the relatively unperturbed study of dynamic molecular interactions and intracellular compartmentation [3,7–12]. Conventional solution-state ^{1}H NMR spectral analysis of tissue extracts (as described previously) requires extensive sample preparation, involving the destruction of the subcellular and molecular organisation within the tissue. Protein precipitation and removal of the cellular lipid provides a purely aqueous sample containing only those hydrophilic species within the cytosol and other aqueous-based matrices. In this instance, the approach is useful for the detection of low molecular weight hydrophilic metabolites. Chloroform/methanol extracts of tissue allows a complementary range of hydrophobic compounds to be measured which are not found in aqueous extracts and come from a variety of subcellular compartments with different degrees of motional freedom.

The MAS-NMR enables the study of the intact *ex vivo* state of a tissue and the spectra have contributions from hydrophobic and hydrophilic substances. Enzymic processes can also be studied using MAS-NMR spectra of tissues, e.g. the selective deuteration of alanine by alanine aminotransferase [7,8]. Furthermore, MAS-NMR can also provide the means to investigate molecular compartmentation, for example, by employing differential spin speeds it is possible to increase the spectral contributions from more compartmentalised species [8] or by the use of magic angle field gradients differentially motionally constrained species can be investigated [12]. Since MAS-NMR spectroscopy requires a much smaller sample size than that needed to produce a tissue extract, thus enabling the study of needle biopsy samples. The nondestructive nature of this technique also provides the potential for studying histopathology on a sample following MAS-NMR experiments potentially leading to direct tissue structure-function correlations [21].

3.2. ^{1}H (MAS-) NMR spectroscopic analyses of intact and extracted liver following ANIT treatment

The PCA of aqueous ^{1}H NMR spectra showed time-dependent alterations in the levels of endogenous metabolites following ANIT treatment (Figs. 2 and 3). These included a, subtle but progressive, reduction in the

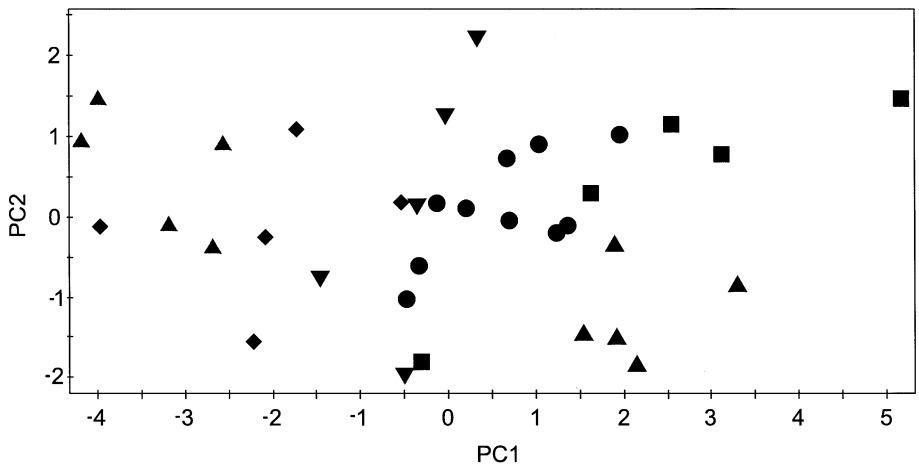

Fig. 5. PC map showing the mapping position of aqueous liver tissue extract ^{1}H NMR spectra (aromatic region δ 6.0–10.0) obtained from individuals following treatment with corn oil (●) or ANIT at various time-points postdose: 3 hr (blue), 7 hr (green), 24 hr (purple), 31 hr (red), and 16 hr (orange). Principal components 1 and 2 explain 82% of the data variance.

intensity of glycogen and glucose signals from 3 to 31 hr p.d., which recovered to control levels by 168 hr p.d., an increase in choline and phosphocholine concentrations from 3 to 168 hr p.d., raised lactate at 24–31 hr p.d. and the appearance of the C18 bile acid methyl signal at 24–31 hr p.d. Closer inspection of the spectra revealed augmented glutathione levels at 24 hr p.d. (Fig. 2).

PCA analysis of the selected aromatic region (δ 6.0–10.0) of the aqueous liver extracts revealed a number of ANIT-induced biochemical perturbations (Figs. 4 and 5). At 3–24 hr p.d., an increase in inosine signals was observed. At 24–168 hr p.d., elevated levels of uridine, uracil, adenine, adenosine, nicotinuric acid and the monophosphates of guanosine and thymidine (5′ GMP and 5′ TMP) were observed. Furthermore, tyrosine, histidine, and phenylalanine increased at 168 hr, fumarate decreased at 31 hr and an unassigned multiplet (δ 6.7) appeared transiently at 24 hr p.d. ^{1}H NMR spectra of chloroform/methanol liver

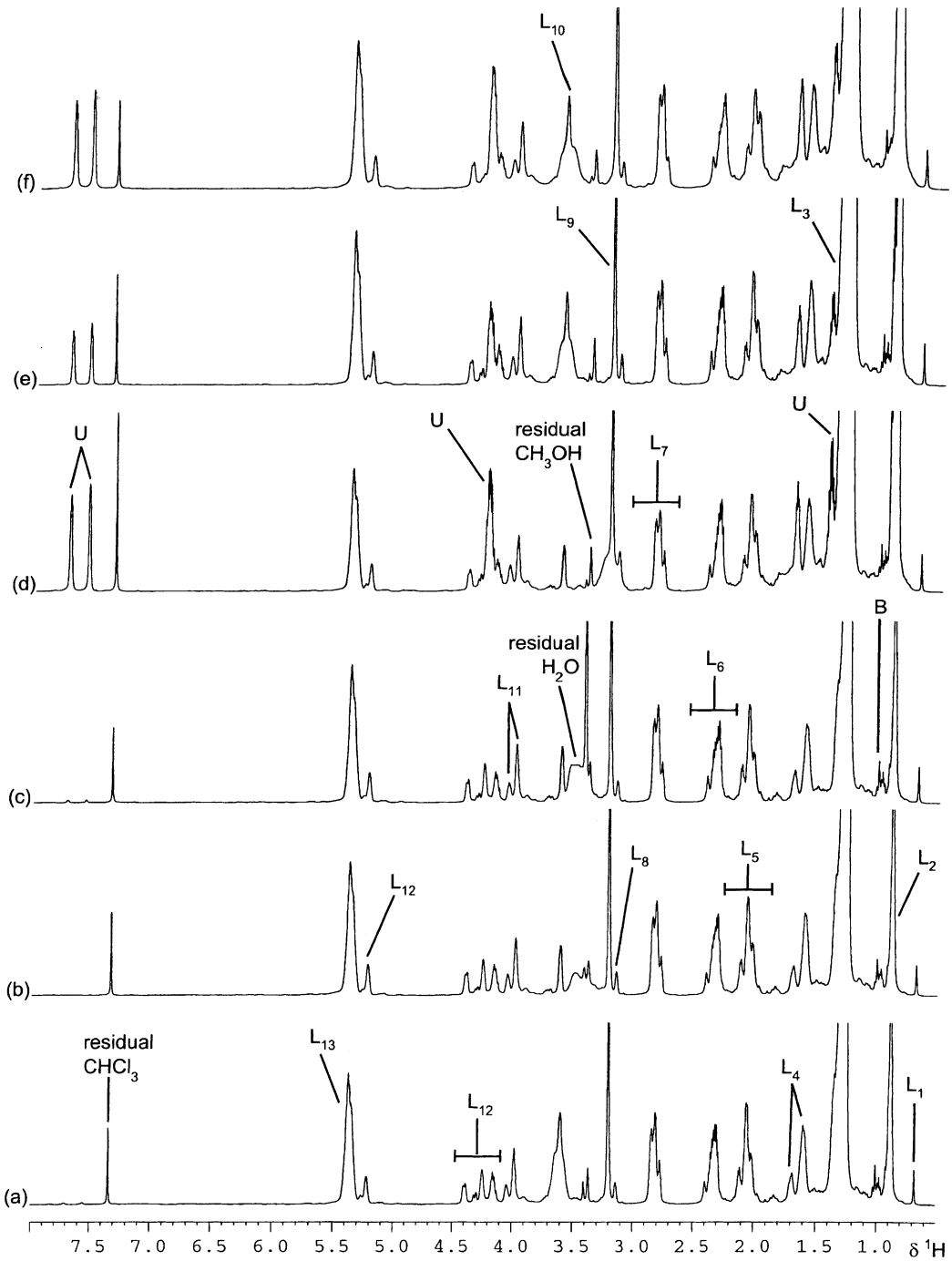

Fig. 6. Series of 600 MHz single pulse ^{1}H NMR spectra (δ 0.5–8.0) of liver tissue chloroform/methanol extracts (left lateral lobe) at various time-points following the administration of ANIT (150 mg/kg): (a) control, (b) 3 hr, (c) 7 hr, (d) 24 hr, (e) 31 hr, and (f) 168 hr postdose. Key: As for Fig. 1 with the following additions U, unassigned signals tentatively identified as lipid hydroperoxide/conjugated diene or imidazole species.

tissue extracts showed a number of treatment-related changes in metabolite levels (Figs. 6 and 7). At 24–168 hr p.d., there was an increase in many of the lipid signals including the terminal methyl (δ 0.9) and methylene groups (δ 1.3), a change in the ratio of the two $CH_2{}^*CH_2CO$ signals at δ 1.6 and 1.7 and the appearance of unknown signals at δ 1.42 (m), 4.22 (m) and at δ 7.56 (s), 7.71(s).

The ^{1}H MAS-NMR spectra of intact liver acquired at various time-points after the administration of ANIT showed marked and consistent changes in the levels of endogenous metabolites from 7 hr p.d. onwards (Fig. 8). The predominant changes identified in the PCA analysis (Fig. 9) included an increase in the signal intensities of triglycerides at 24 and 31 hr p.d., which fell to below control levels at 168 hr p.d. and a reduction in the intensity of glucose and glycogen resonances between 3 and 31 hr p.d. before recovery to control levels at 168 hr p.d. This was accompanied by elevated trimethylamine-*N*-oxide (TMAO), betaine, phosphocholine, and choline signals in all but one individual at 168 hr p.d. On closer inspection of the ^{1}H MAS-NMR spectra, a slight increase in the bile acid C18 methyl signal (δ 0.7) at 24 and 31 hr p.d. was observed and in some individuals, a moderate elevation in the resonances from the amino acids leucine and isoleucine at 24–31 hr p.d.

The majority of the ANIT-induced biochemical perturbations detected by ^{1}H NMR-PR analysis of aqueous extracts were also found in the ^{1}H MAS-NMR spectra of intact liver, with the exception of changes in lactate and glutathione. The increase in choline and phosphocholine over the entire time-course in the ^{1}H NMR spectra of aqueous liver tissue extracts was not observed in the ^{1}H MAS-NMR spectra. It is possible that the extraction procedure had released these species from a highly constrained motional environment (which would give dipolar couplings greater than the spin rate, ν_r, e.g. membranous) within the cellular matrix, into solution where an isotropic motion had enabled their measurement by liquid state ^{1}H NMR spectroscopy. The elevated levels of choline and phosphocholine maybe products of membrane breakdown and lipid catabolism as a result of the action of ANIT, which in the solid tissue contributed to the obstruction of the bile ducts resulting in a constrained molecular motion.

^{1}H NMR-PCA of the aqueous liver extracts also identified a rise in the free nucleosides inosine, adenosine, and uridine together with free adenine, uracil, and the

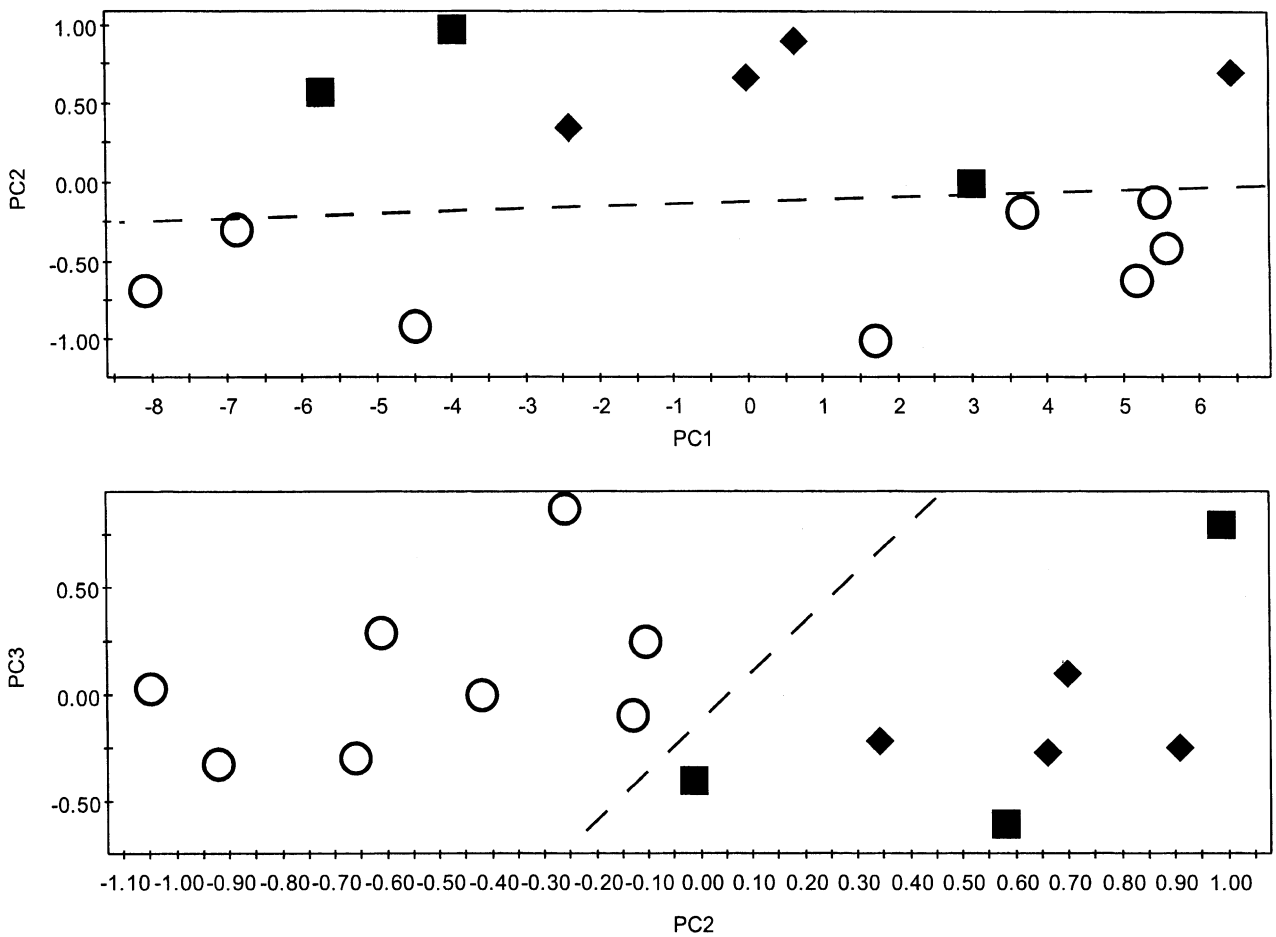

Fig. 7. PC maps showing the mapping position of chloroform/methanol liver tissue extract ^{1}H NMR spectra obtained from individuals following treatment with corn oil (open circles) or ANIT at 24 hr (■) and 31 hr (◆) postdose. Principal components 1, 2, and 3 explain 99.3% of the data variance. No PCA separation was observed at 3, 7, and 168 hr postdose.

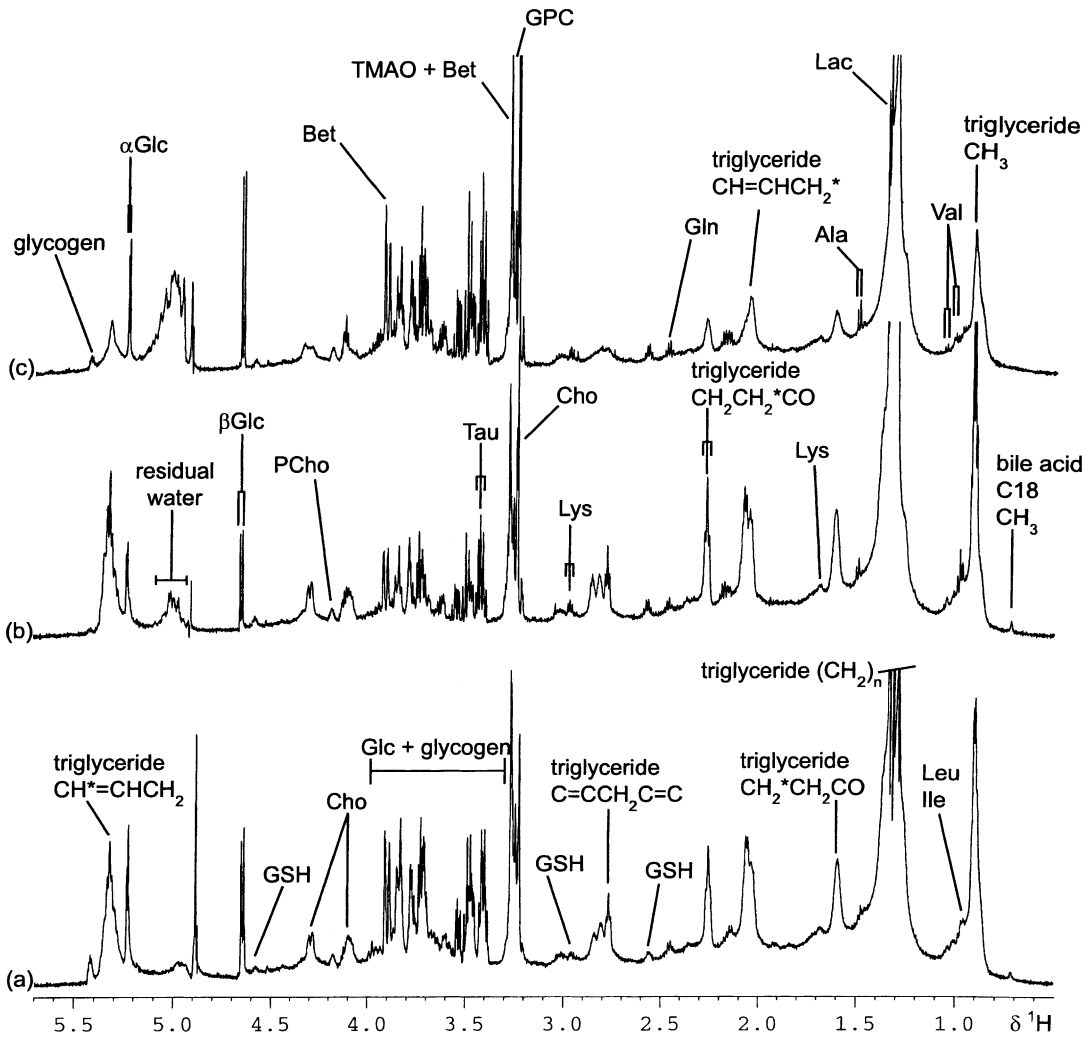

Fig. 8. Series of 600 MHz single pulse ^{1}H MAS-NMR spectra (δ 0.5–5.7) of the left lateral lobe of the liver at various time-points following the administration of ANIT (150 mg/kg): (a) control, (b) 31 hr, and (c) 168 hr postdose. Lorentzian–Gaussian resolution-enhancement (LB = −2, GB = 0.3) was applied to all spectra. Key: As for Fig. 1 with the following additions Bet, betaine; Tau, taurine.

nucleotide 5′ monophosphates GMP and TMP. It is possible that ANIT metabolites or the parent compound could mimic purine and pyrimidine bases with consequent inhibition of enzymes involved in nucleotide metabolism [22]. The observed increase in nicotinuric acid, an excretory metabolite of nicotinate, suggests inhibition of coenzyme biosynthesis, which could be manifested by ANIT in a similar manner to that described for the nucleotide enzymes. The rise in tyrosine, histidine, and phenylalanine at 168 hr coincides with pathological observation of bile duct hyperplasia and these may represent biomarkers of this proliferative response. Decreased fumarate at 31 hr p.d. indicates altered citric acid cycle metabolism.

Although both ^{1}H NMR-PR analysis of lipidic extracts and ^{1}H MAS-NMR-PR of intact liver identified an increase in lipid signals at 24–31 hr p.d., both methods produced contradictory results at 168 hr p.d. MAS-NMR spectra showed a decrease in triglyceride resonances to below control levels whilst NMR spectra of chloroform/methanol extracts showed a rise at this time-point. This may have occurred as a consequence of the extraction procedure, releasing a species previously in a constrained motional environment. If this is the case, it suggests an ANIT-induced redistribution of cellular lipid. Solid samples usually exhibit anisotropic dipolar couplings in NMR spectra (partially reduced by the MAS experiment) and restricted molecular mobility, which in the solution state do not exist due to the averaging nature of isotropic motion and the lack of metabolite compartmentation. ^{1}H NMR-PCA analysis of chloroform/methanol liver extracts identified a number of signals arising from unknown metabolites not observed in the ^{1}H MAS-NMR PCA analysis, which may have originated in a motionally restricted environment, prior to extraction into solution. These unknown metabolites may include a lipid hydroperoxide or conjugated diene formed as a result of ANIT-induced lipid peroxidation [23–25]. Alternatively, it may be an endogenous imidazole species elevated as a consequence of ANIT-treatment, as the aromatic signals alone are indicative of such a moiety. Certain imidazole derivatives

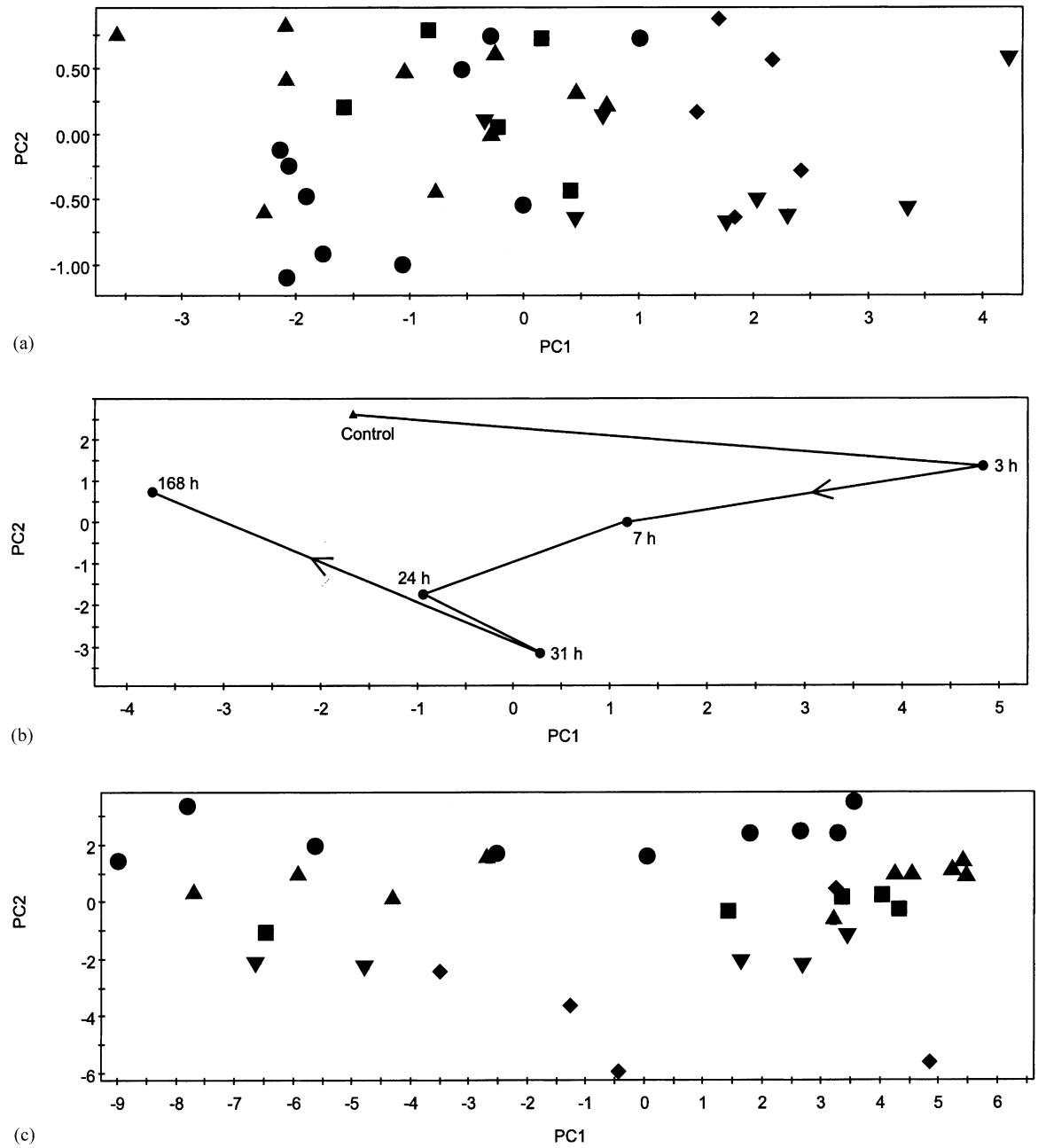

Fig. 9. (a) PC map showing the mapping position of intact liver single pulse ^{1}H MAS-NMR spectra obtained from individuals following treatment with corn oil (●) or ANIT at various time-points postdose: 3 hr (blue), 7 hr (green), 24 hr (purple), 31 hr (red), and 168 hr (orange). (b) PCA metabolic trajectory plot mapping the average position for each time-point as a function of the ^{1}H NMR spectra from both aqueous and chloroform/methanol extracts of liver. (c) PC map showing the mapping position of individuals following treatment with corn oil (●) or ANIT at various time-points postdose: 3 hr (blue), 7 hr (green), 24 hr (purple), 31 hr (red), and 168 hr (orange) as a function of the ^{1}H NMR spectra from both aqueous and chloroform/methanol extracts of liver. Principal components 1 and 2 explain 91% of the data variance.

are known to induce various phase II drug metabolising enzymes including, 1-naphthol glucuronosyltransferase [26], and it may be the case that levels of an endogenous species are increased in order to induce rapid and efficient removal of ANIT metabolites.

The combined PCA analysis of the aqueous and lipophilic tissue extract spectra resulted in time-dependent clustering and separation as a result of changes in those metabolites also identified in the separate ^{1}H NMR-PCA analysis of each extract (Fig. 9b and c). However, the combined PCA of tissue extracts indicates recovery at 168 hr (mapping nearest control) whilst the MAS-NMR-PCA suggests this is not the case, with 168 hr p.d. mapping from control (Fig. 9a). The MAS-NMR data gives the better clustering of data points by PCA. The combined extract NMR-PCA data suffers from large variation within groups and time-points including controls, emphasised in PC1. The MAS-NMR detected biochemical differences at 168 hr (TMAO, betaine, choline and phosphocholine) coincide with the bile duct hyperplasia lesion observed by histopathology. As such, MAS-NMR

spectroscopy provides an effective tool, providing a direct correlation with histopathological data, not suffering metabolite losses as a consequence of the sample preparation. At present, high throughput automation of MAS-NMR spectroscopy is not possible for tissue samples due to sample preparation and biochemical stability issues [7]. However, recent technological advances in spectrometer hardware should make automation of MAS-NMR spectroscopy a real possibility in the near future.

Each of the ^{1}H NMR spectroscopic analyses of extracts identified one or two of the well-documented ANIT-induced biochemical perturbations in liver tissue including steatosis, bile duct obstruction and altered glucose and glycogen metabolism. However, it was ^{1}H MAS-NMR analysis of intact liver tissue that was able to detect all of the reported ANIT-induced metabolic effects. The ability to measure and detect a multitude of tissue metabolites, with minimal disruption to the system and without metabolite discrimination, makes this technique a potentially powerful tool for the study of drug-induced damage, disease diagnosis and aetiology.

4. Conclusion

This work has illustrated the potential of high resolution ^{1}H MAS-NMR spectroscopy (coupled with pattern recognition techniques) to probe the biochemistry of *ex vivo* intact biological tissues compared to the laborious and discriminatory process of producing tissue extracts for ^{1}H NMR spectroscopic analysis. Therefore, ^{1}H MAS-NMR spectroscopy offers a more efficient means of investigating drug-induced tissue damage and disease aetiology, with the added capability of disease diagnosis.

References

[1] Waters NJ, Holmes E, Williams A, Waterfield CJ, Farrant RD, Nicholson JK. NMR and pattern recognition studies on the time-related metabolic effects of α-naphthylisothiocyanate on liver, urine and plasma in the rat: an integrative metabonomic approach. Chem Res Toxicol 2001, in press.

[2] Garrod S, Humpfer E, Connor SC, Connelly JC, Spraul M, Nicholson JK, Holmes E. High resolution ^{1}H NMR and magic angle spinning NMR spectroscopic investigation of the biochemical effects of 2-bromoethanamine in intact renal and hepatic tissue. Magn Reson Med 2001;45(5):781–90.

[3] Griffin JL, Walker LA, Troke J, Osborn D, Shore RF, Nicholson JK. The initial pathogenesis of cadmium induced renal toxicity. FEBS Lett 2000;478:147–50.

[4] Cheng LL, Ma MJ, Becerra L, Ptak T, Tracey I, Lackner A, Gonzalez RG. Quantitative neuropathology by high resolution magic angle spinning proton magnetic resonance spectroscopy. Proc Natl Acad Sci USA 1997;94:6408–13.

[5] Tomlins AM, Foxall PJD, Lindon JC, Lynch MJ, Spraul M, Everett JR, Nicholson JK. High resolution magic angle spinning ^{1}H NMR analysis of intact prostatic hyperplastic and tumour tissues. Anal Comm 1998;35:113–5.

[6] Andrew ER, Eades RG. Removal of dipolar broadening of NMR spectra of solids by specimen rotation. Nature 1959;183:1802.

[7] Waters NJ, Garrod S, Farrant RD, Haselden JN, Connor SC, Connelly JC, Lindon JC, Holmes E, Nicholson JK. High-resolution magic angle spinning ^{1}H NMR spectroscopy of intact liver and kidney: Optimisation of sample preparation procedures and biochemical stability of tissue during spectral acquisition. Anal Biochem 2000;282:16–23.

[8] Garrod S, Humpfer E, Spraul M, Connor SC, Polley S, Connelly JC, Lindon JC, Nicholson JK, Holmes E. High resolution magic angle spinning ^{1}H NMR spectroscopic studies on intact rat renal cortex and medulla. Magn Reson Med 1999;41:1108–18.

[9] Bollard ME, Garrod S, Holmes E, Lindon JC, Humpfer E, Spraul M, Nicholson JK. High resolution ^{1}H and ^{1}H-^{13}C magic angle spinning NMR spectroscopy of rat liver. Magn Reson Med 2000;44:201–7.

[10] Humpfer E, Spraul M, Nicholls AW, Nicholson JK, Lindon JC. Direct observation of resolved intracellular and extracellular water signals in intact human red blood cells using ^{1}H MAS NMR spectroscopy. Magn Reson Med 1997;38:334–6.

[11] Millis KK, Maas WF, Cory DG, Singer S. Gradient high resolution magic angle spinning NMR spectroscopy of human adipocyte tissue. Magn Reson Med 1997;38:399–403.

[12] Griffin JL, Troke J, Walker LA, Shore RF, Lindon JC, Nicholson JK. The biochemical profile of rat testicular tissue as measured by magic angle spinning ^{1}H NMR spectroscopy. FEBS Lett 2000;486:225–9.

[13] Goldfarb S, Singer EJ, Popper H. Experimental cholangitis due to alpha-naphthylisothiocyanate (ANIT). Am J Pathol 1962;40:685–98.

[14] Zimmerman HJ. Drug-induced liver disease. Drugs 1978;16:25–45.

[15] Plaa GL, Priestly BG. Intrahepatic cholestasis induced by drugs and chemicals. Pharmacol Rev 1976;28:207–73.

[16] Farrant RD, Lindon JC, Nicholson JK. Internal temperature calibration for ^{1}H NMR spectroscopy of blood plasma and other biofluids. NMR Biomed 1994;7:243–7.

[17] Holmes E, Foxall PJD, Nicholson JK, Neild GH, Brown SM, Beddell CR, Sweatman BC, Rahr E, Lindon JC, Spraul M, Neidig P. Automatic data reduction and pattern recognition methods for analysis of ^{1}H nuclear magnetic resonance spectra of human urine from normal and pathological states. Anal Biochem 1994;220:284–96.

[18] Beebe KR, Pell RJ, Seahsholt MB. Chemometrics: a practical guide. New York: Wiley, 1998.

[19] Beckwith-Hall BM, Nicholson JK, Nicholls AW, Foxall PJD, Lindon JC, Connor SC, Abdi M, Connelly JC, Holmes E. Nuclear magnetic resonance spectroscopic and principal components analysis investigations into biochemical effects of three model hepatotoxins. Chem Res Toxicol 1998;11:260–72.

[20] Lindon JC, Nicholson JK, Holmes E, Everett JR. Metabonomics: metabolic processes studied by NMR spectroscopy of biofluids. Concepts Magn Reson 2000;12:289–320.

[21] Cheng LL, Wu C, Smith MR, Gonzalez RG. Non-destructive quantitation of spermine in human prostate tissue samples using HRMAS ^{1}H NMR spectroscopy at 9.4 T. FEBS Lett 2001;494:112–6.

[22] Sneider TW, Krawitt EL, Potter VR. Selected enzymes of pyrimidine nucleotide metabolism in livers from rats fed α-naphthylisothiocyanate. Cancer Res 1970;30:44–7.

[23] Sparling ML, Zidovetzki R, Muller L, Chan SI. Analysis of membrane lipids by 500 MHz ^{1}H NMR. Anal Biochem 1989;178:67–76.

[24] Pollesello P, Eriksson O, Kvam BJ, Paoletti S, Saris NL. ^{1}H NMR studies of lipid extracts of rat liver mitochondria. Biochem Biophys Res Comm 1991;179(2):904–11.

[25] Ohta Y, Kongo M, Sasaki E, Harada N. Change in hepatic antioxidant defence system with liver injury development in rats with a single α-naphthylisothiocyanate intoxication. Toxicology 1999;139:265–75.

[26] Ritter JK, Franklin MR. Induction of hepatic oxidative and conjugative drug metabolism in the hamster by *N*-substituted imidazoles. Toxicol Lett 1987;36(1):51–9.